ELSEVIER

Polymer 44 (2003) 2403–2410

polymer

www.elsevier.com/locate/polymer

An atomic force microscopy study of ozone etching of a polystyrene/polyisoprene block copolymer

S. Collins, I.W. Hamley*, T. Mykhaylyk

Department of Chemistry, University of Leeds, Leeds LS2 9JT, UK

Received 12 August 2002; received in revised form 17 December 2002; accepted 4 February 2003

Abstract

The ozone etching of a commercial poly(styrene)/poly(isoprene) (PS/PI) block copolymer (Kraton D1117) was studied by atomic force microscopy. The copolymer contains 17% PS and forms a cylindrical phase in the melt. The copolymer dewetted when spin coated onto a silicon wafer but the film was stable on a grown silicon oxide layer. The structure of the stripe pattern formed was examined on substrates with different oxide layer thicknesses (surface energies). Finally etching by ozone was investigated. For low ozone doses, no degradation of polymer was observable. Extended ozone treatment resulted in more obvious degradation, but the etching was non-selective.

Keywords: Triblock copolymers; Ozonation; Atomic force microscopy

1. Introduction

Interest in block copolymer thin film structures is expanding rapidly due to potential exciting nanotechnology applications. These include the fabrication of high density magnetic data storage media [1–3], nanoelectrode arrays [4], diamond nanocolumn arrays [5], the templating of metal nanowires [6,7] and the lithographic patterning of semiconductors with ultrasmall feature sizes [8,9]. Reviews of structure formation in block copolymer films are available [10–12]. Nanotechnology applications have also been discussed [13].

Here, surface etching of a commercial poly(styrene)/poly(isoprene) (PS/PI) block copolymer by ozonolysis is studied by atomic force microscopy (AFM) and ellipsometry. The polymer studied is a Kraton thermoplastic elastomer, comprising two thirds PS–PI–PS triblock and one third PS–PI diblock [14]. The blend contains 17% PS and forms a hexagonal phase of PS cylinders in a PI matrix in the melt. In thin films, stripe or dot patterns are expected depending on whether the PS cylinders lie parallel or perpendicular to the substrate, respectively. The surface tension of PI ($\gamma = 32$ mN m^{-1}, 20 °C) [15] is lower than that of PS ($\gamma = 40$ mN m^{-1}, 20 °C), [15] and therefore a top layer of PI is expected. Based on the results of careful force–distance AFM curve measurements by Krausch and coworkers [16] for an analogous PS–PB–PS (PB = polybutadiene) triblock, we expect the film structure to be as shown in Fig. 1. The buried glassy PS cylinders lead to apparent height variations in AFM topography images, even when the PI surface is flat as it is before etching [16].

Ozone etching of poly(isoprene) or poly(butadiene) in block copolymers with a poly(styrene) matrix has previously been employed by Harrison and coworkers to fabricate masks with holes or stripes for pattern transfer onto semiconductors via reactive ion etching [8,9]. Here we investigate the etching of the inverse structure with a poly(isoprene) matrix. We also study a commercially available (majority triblock) copolymer, in contrast to Harrison et al. who employed model diblocks synthesized in-house. The change in morphology as a function of ozone dose is examined by AFM. The conditions to obtain a well-defined initial stripe morphology were carefully investigated, in particular the effect of substrate surface energy (via thermally grown silicon oxide layers of controlled thickness) on the morphology of spin-cast films was examined by AFM.

* Corresponding author. Tel.: +44-113-343-6430; fax: +44-113-343-6565.

E-mail address: I.W.Hamley@chem.leeds.ac.uk (I.W. Hamley).

0032-3861/03/$ - see front matter © 2003 Elsevier Science Ltd. All rights reserved.
doi:10.1016/S0032-3861(03)00113-7

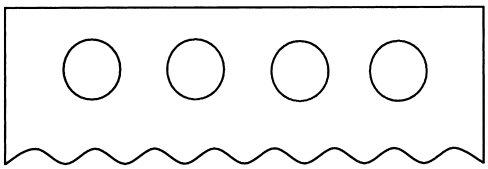

Fig. 1. Schematic diagram of PS–PI–PS triblock as cast onto a silicon wafer.

2. Experimental

2.1. Materials

Kraton D1117 was obtained from Kraton Polymers (Chester, UK). It is a commercial PS/PI copolymer containing 17% PS and 83% PI [17]. The polymer contains 33% PS–PI diblock and 67% PS–PI–PS triblock. The molecular weight was determined by Rapra Technology (Shrewsbury, UK) using GPC with THF and a triple detector, against polystyrene standards. Two components were observed—approx 80,000 g mol^{-1} (~40%) and 150,000 g mol^{-1} (~60%) respectively, corresponding to the diblock and triblock, respectively. SAXS (Daresbury, UK) revealed the structure of annealed D1117 to be hexagonal-packed cylinders, with bulk domain spacing of 27.6 ± 0.3 nm. Silicon wafers with a surface perpendicular to ⟨111⟩ were obtained from Prolog Semicor (Kiev, Ukraine).

2.2. Wafer and film preparation

Silicon wafers were oxidised by heating at 1100 °C in a furnace (Lenton Thermal Designs Ltd, Market Harborough, UK) for the required period of time. Thin films (approximate thickness 100 nm) were obtained through spin coating at 2500 rpm from 2 wt% toluene solutions on bare or oxidised silicon wafers. The wafers were cleaned by rinsing with toluene immediately before spin coating [18]. The film morphology was examined after annealing in a vacuum oven at 130 °C (i.e. above the glass transition temperature of PS) for various times (0, 3, 6 and 24 h). The thickness of the oxide layer on the surface was measured by ellispsometry and found to increase with time of heat treatment from 2.3 nm (0 h) to 241 nm (6 h) (Table 1).

We found that Kraton polymer films spin coated using our cleaning procedure wet a silicon wafer with a thermally grown oxide better than wafers with native oxide. It is well known that a silicon surface covered by a native oxide layer is generally contaminated by organic and other impurities [19,20] if a special cleaning procedure has not been performed. The possible explanation of the better wettability of the thermally grown oxide silicon surface is the removal of organic impurities under high temperature. To characterize the difference between these two types of substrates quantitatively a contact angle technique was employed followed by surface energy calculation.

Table 1
Thickness of oxide layer (obtained by ellipsometry) and surface energies (obtained by contact angle) after oxidation of the silicon wafer at 1100 °C for the times indicated

Time (h)	Thickness of oxide layer (nm)	Surface energy (mJ m^{-2})
0	2.3	49.3
1	88	54.7
2	141	58.1
6	241	–

The surface energy of the wafers with grown oxide layers was calculated from contact angle measurements performed by the sessile drop method [21]. The contact angles of water purified by a Milli-Q™ water system and diiodomethane of 99% purity (Aldrich) were measured. Each contact angle value was the average from measurements on at least 10 drops (both sides). The surface energy γ_s was calculated using the geometric method [22]:

$$(1+\cos\theta)/\gamma_{lv} = 2\sqrt{\gamma_s^d \gamma_{lv}^d} + 2\sqrt{\gamma_s^p \gamma_{lv}^p}$$

where θ is the measured contact angle of the test liquid, γ_{lv}, γ_{lv}^d and γ_{lv}^p are the known liquid–vapour surface energy of the liquid and its dispersion and polar component, respectively, and γ_s^d and γ_s^p are the dispersion and polar components of the tested substrate, respectively.

The total surface energy of silicon wafers with native oxide was found to be 49.3 mJ m^{-2} (Table 1) whereas oxidation in the furnace under the 1100 °C temperature increases the total surface energy e.g. for 1 h it has risen to 54.7 mJ m^{-2}. These data demonstrate that the silicon surface with thermally grown oxide has a higher surface free energy than does the silicon surface covered by native oxide and as a result thermally treated silicon wafers are more hydrophilic and have better wettability properties.

2.3. Ozonation

Ozone was generated using an ozone generator (model 502, Fischer Technology, Bonn, Germany). The resulting oxygen/ozone mixture was passed through a diffuser, producing a stream of bubbles across the sample, which was fastened to a Teflon stage in a glass reactor cell [9]. The reactor cell was filled with deionised water (~3 l) to promote removal of polydiene fragments during ozonation. During reaction, ozone cleaves carbon–carbon double bonds [23], producing low molar mass products that can be removed by water. At the same time, PS is cross-linked by ozone. After passing oxygen/ozone through the reaction cell, at ambient temperature for various periods of time, it was flushed with oxygen for five minutes before the coated wafers were removed, the edges of the wafers were touched with tissue to wick away the remaining water and the wafers were left to dry overnight in a desiccator. The production of ozone depends on the flow of oxygen and the power setting. These were adjusted to give a flow of 2.5 l min^{-1} oxygen

containing (according to the performance data supplied by the manufacturer) ~0.1% wt/wt ozone.

2.4. Atomic force microscopy

The sample surfaces were investigated using a Digital Instruments multimode AFM with a Nanoscope IIIa controller. Topographic and phase images were recorded simultaneously using tapping mode with Si tips. The topographic and phase mages were very similar so only the topographic images are presented as this enables discussion of the apparent height variations in the surface morphology.

2.5. Ellipsometry

A computer controlled phase-modulated spectroscopic ellipsometer (Beaglehole Instruments, New Zealand) with a polarizer-birefringence modulator-sample-analyser (P-BM-S-A) configuration was employed for silicon oxide film thickness determination. A one layer model (comprising silicon substrate–silicon oxide film–air) with flat boundaries was used to fit the experimental data. Tabulated data for the optical constants of silicon and silicon oxide were used [24].

3. Results and discussion

3.1. Structure of copolymer

Thin films of the copolymer D1117 were cast onto silicon wafers and then annealed at 130 °C for 3 h. Ellipsometry indicated a polymer film thickness of approximately 100 nm. This corresponds to approximately 3.5 layers (as the bulk domain spacing for D1117 was found by SAXS to be 27.6 nm). Fig. 2a shows the topographic AFM image for the 3 h annealed sample on the native silicon oxide substrate. For samples with a thin oxide layer (short oxidation time) there was evidence for dewetting after 6 h annealing. This dewetting is not the focus of the current paper, and is not considered further.

In order to increase the substrate surface energies, silicon was heated in a furnace to increase the thickness of the surface oxide layer [20]. Fig. 2b shows the topographic AFM image of a sample cast onto silicon that had been heated at 1100 °C for 1 h (without further annealing). This reveals a worm-like pattern which suggests the formation of PS cylinders. These appear either to be not fully developed, or the orientation may not be completely parallel to the substrate. Depth profiling to determine cylinder orientation within the film [25] was not attempted.

Subsequently a systematic study of the effect of the thickness of the oxide layer (controlled by varying the time the silicon spent in the furnace) on the morphologies of spin coated thin films was undertaken.

Thin films of the triblock were cast onto silicon wafers which had been previously heat-treated at 1100 °C for 1, 2 or 6 h. These samples were then annealed at 130 °C for 3 h (Fig. 3). For the 1 h heat treated silicon wafer a stripe pattern akin to a finger print is observable (Fig. 3a).

For both the 2 h (Fig. 3b) and the 6 h (Fig. 3c) heat treated silicon wafers a stripe pattern akin to a finger print is also observable after annealing. In the following investigation of ozonation of the copolymers, polymer films on wafers with 1 h oxide growth were employed.

3.2. Ozonation of copolymer

Thin films of the copolymer were cast onto oxide coated silicon wafers and then annealed at 130 °C for 3 h before being subjected to ozonation. AFM topography images of films obtained after increasing doses of ozone are shown in Fig. 4. Cross section line profiles are shown in Fig. 5 and information on stripe spacing and depth are listed in Table 2. After 5–10 min ozone treatment, no disordering of the initial stripe pattern was observed (Fig. 4b). After 15 min (Fig. 4c) the morphology is still similar to the initial pattern (Fig. 3a), although with a larger number of defects (disclinations). The finger print nature of the pattern results in different portions of the pattern having different spacings between stripes. Consider, for example, the untreated film (Fig. 5a and b and Table 2). In the main portion of the image (top left hand corner, Fig. 5a), the average stripe spacing (measured between the two arrows) is 47.6 nm. For the minor portion of the same image (bottom left hand corner, Fig. 5b) the average interval spacing is 29.3 nm.

After 25 min ozonation the influence of etching is obvious as the stripe order is reduced to give a worm-like morphology (Fig. 4d, which may be compared to Fig. 2b). Cross section data (Fig. 5c and Table 2) indicate an increase in stripe spacing. This is more pronounced after 50–80 min ozonation (Fig. 4e and f). It is difficult to obtain a reliable estimate of the domain spacing after 80 min ozonation. Comparing Fig. 5d with Fig. 5c it is apparent that extended ozonation has led to further etching with only isolated peaks present rather than incomplete stripes.

Rather than analysis of cross sections, domain spacings in poorly ordered structures are better analysed by Fourier transform (FT) methods. The domain spacings in the thin films were thus obtained by Fourier transformation of the AFM image. The FT of the topographic images in Fig. 4 revealed two equally spaced rings for 0–15 min ozonation. The radius of the rings changed only very little with etching time, although this was difficult to quantify. For 25–50 min ozonation only one diffuse ring was observable whilst for the 80 min ozonation no ring was observable in the FT image. Rather than relying on the FT data, the change in stripe spacing was quantified through the 2D isotropic power spectral density (PSD) (Fig. 6). Since the rings in the FT were not always circular, anisotropy can influence the amplitude of the peaks in the PSD data, which are thus not

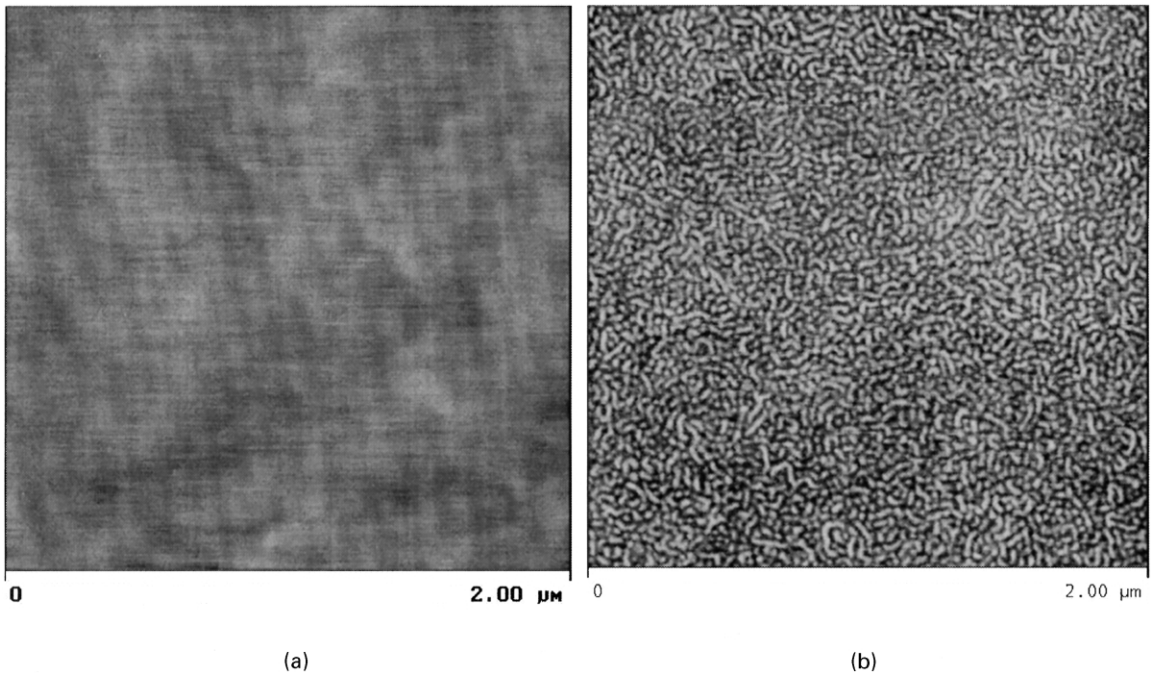

Fig. 2. (a) Topographic AFM images of D1117 cast onto silicon after annealing for 3 h at 130 °C. (b) Topographic AFM images of D1117 cast onto silicon (oxide growth treatment for 1 h at 1100 °C). Sample not subsequently annealed.

on an absolute basis. Nevertheless, it is apparent that the pronounced peak at 0.036 nm is lost between 15 and 25 min, to be replaced by a broader, asymmetric peak corresponding to a longer wavelength structure. The decay in intensity of the peak corresponding to the initial stripe pattern is consistent with the non-selective ozonation of the surface, leading ultimately to the loss of stripe order.

The etching by ozone was also illustrated through depth profiles, obtained via a 'depth analysis' available as part of the AFM image analysis software. It accumulates depth data within a specified area (here the whole $2\,\mu m \times 2\,\mu m$ image), and then applies a Gaussian low-pass filter to the data to remove noise. Depth profiles of the topographic AFM images are shown in Fig. 7, where the position of zero depth corresponds to the highest point measured in the AFM image. The measured depth will be influenced for example by the presence of dust particles on the surface. As a consequence the depths measured are not absolute but do still provide for a comparison of the shape of the depth profiles between the different samples. The depth profiles were typically composed of two overlapping peaks at different depth, reflecting two thickness ranges in the films. As mentioned in the Introduction the actual (initial) surface is flat and these height variations are only apparent [16]. Nevertheless considering how they change upon etching can provide qualitative information on the surface depth. Initially ($t = 0$ min) the main peak is at $\sim$4 nm depth with a shoulder at $\sim$3 nm. The peaks move to progressively larger depths, so after 25 min, the peak is at $\sim$14 nm with a shoulder at $\sim$8 nm. The shoulder has almost disappeared at

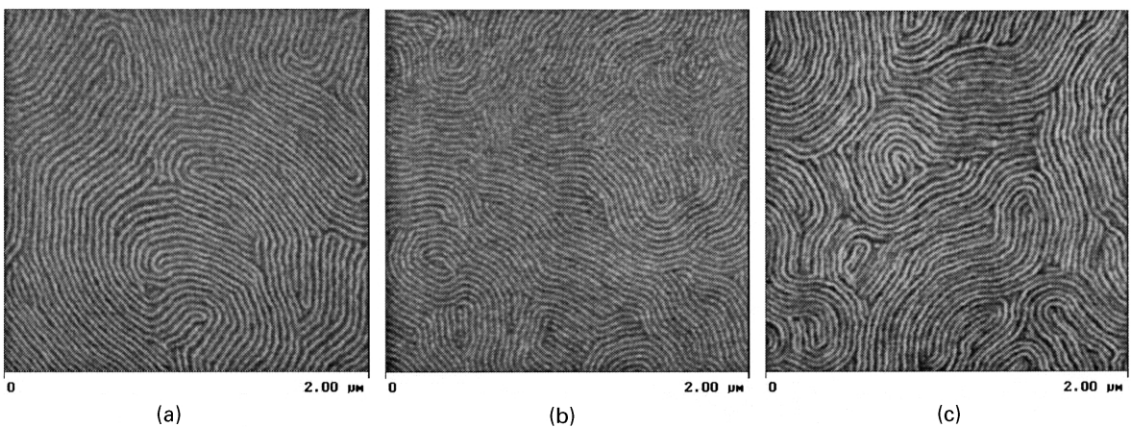

Fig. 3. Topographic AFM images of D1117 cast onto silicon (heat treated at 1100 °C) after annealing for 3 h with polymer: (a) 1, (b) 2, and (c) 6 h silicon oxide growth.

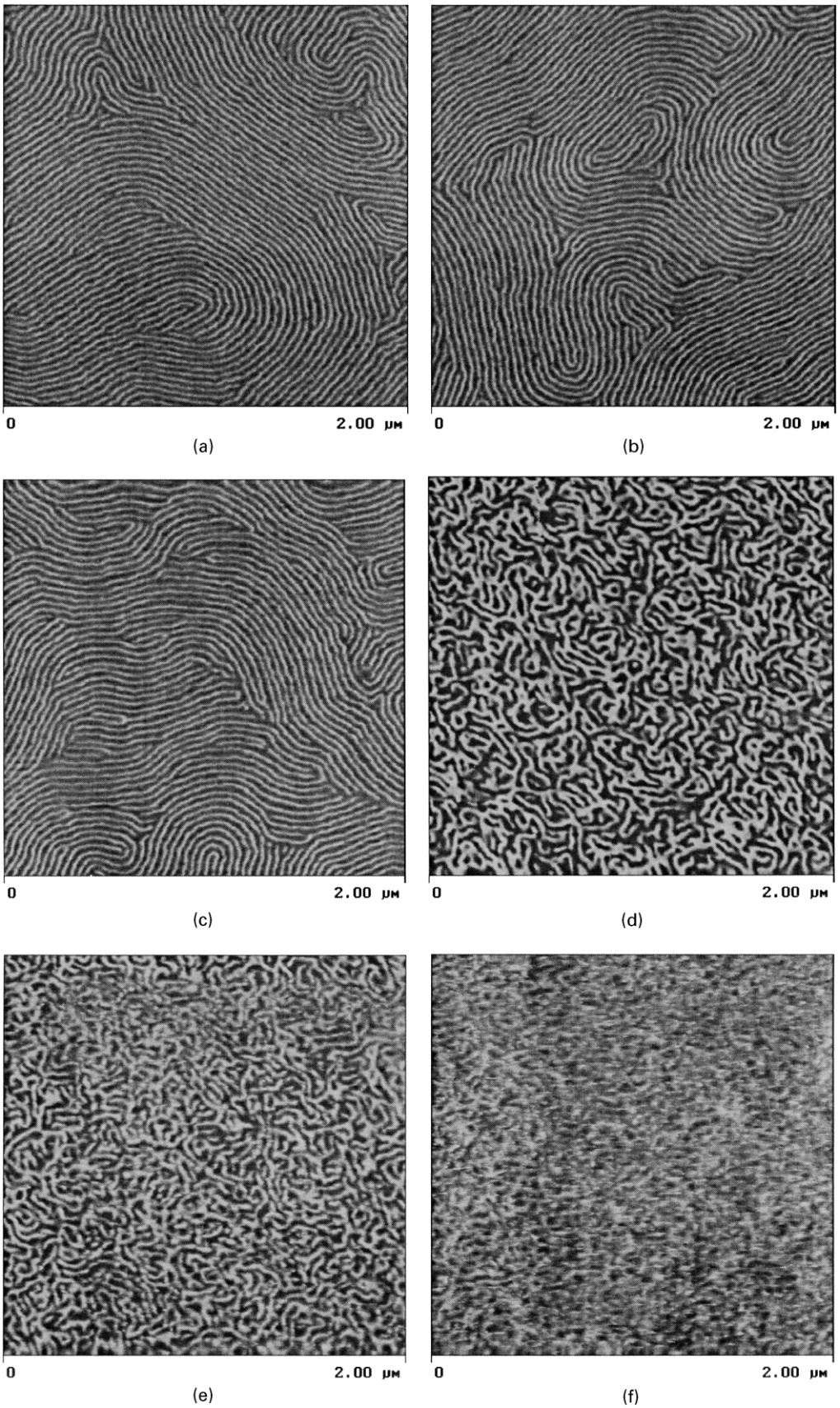

Fig. 4. Topographic AFM images of D1117 cast onto silicon after various times of ozonation (silicon was heat treated for 1 h at 1100 °C before casting, polymer was then annealed at 130 °C for 3 h before ozonation): (a) 5, (b) 10, (c) 15, (d) 25, (e) 50 and (f) 80 min.

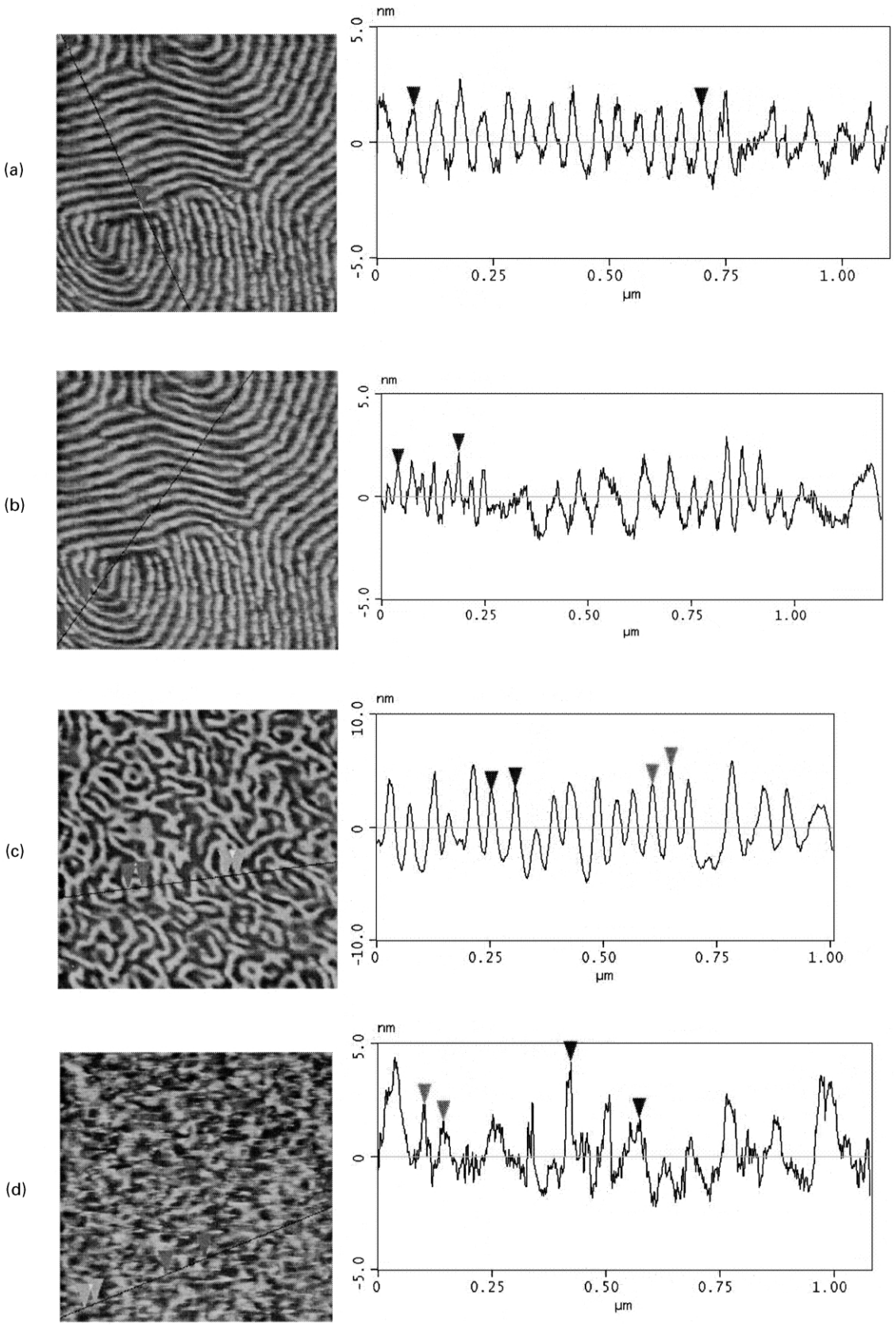

Fig. 5. Topographic AFM images and cross sectional line scans of D1117 cast onto silicon after various times of ozonation (silicon was heat treated for 1 h at 1100 °C before casting, polymer was then annealed at 130 °C for 3 h before ozonation): (a) 0, (b) 0, (c) 25, and (d) 80 min.

Table 2
Interval distances and typical heights for cross section images of topographic AFM images of D1117 cast onto silicon after various times of ozonation (silicon was heat treated for 1 h at 1100 °C before casting, polymer was annealed at 130 °C for 3 h after casting)

Time ozonation (min)	Image	Cross section image	Typical stripe spacings (nm)	Depth peaks (nm)
0	Fig. 2a—stripe	Fig. 5a	47.6	3 (shoulder); 4 (peak)
		Fig. 5b	29.3	–
5	Fig. 4a—stripe	cf Fig. 5a and b	29.1, 36.5	4 (shoulder); 6 (peak)
10	Fig. 4b—stripe	cf Fig. 5a and b	30.7, 38.0	5 (shoulder); 7 (peak)
15	Fig. 4c—stripe	cf Fig. 5a and b	34.2, 40.5	6 (shoulder); 9 (peak)
25	Fig. 4d—partly stripy	Fig. 5c	41.0, 52.7	8 (shoulder); 14 (peak)
50	Fig. 4e—partly stripy	cf Fig. 5c	37.1, 56.6	13 (peak)
80	Fig. 4f—no structure	Fig. 5d	41.0, 75.2	15 (peak)

50 min, while for 80 min only one sharp peak (at ~15 nm) is seen.

Comparing the data obtained by analysis of the AFM images allows an understanding of the etching process to be obtained. Before ozonation the surface is stripy due to the buried glassy PS cylinders. Upon initial ozonation (5–10 min) the PI layer on the surface (estimated thickness 10 nm) starts to be etched. As the underlying PS cylinders are not reached the same stripe pattern appears (Fig. 4a and b), with a similar depth distribution. The situation after 15 min is similar except that the etching has progressed a bit further (as shown by the depth distribution) and the PS cylinders are just starting to be eroded (Fig. 4c). After 25 min the etching has progressed further with all the PS cylinders being eroded at irregular intervals. At 50 min (Fig. 4e) the etching has continued with almost all the covering layer of PI having been removed with the depth distribution being nearly monomodal. After 80 min etching there is no ordered structure left on the surface (Fig. 4f) and the depth distribution (Fig. 6) is a single Gaussian peak which reflects the complete removal of the top PI layer and a random etching of the underlying PI and PS. This indicates that the ozonation has resulted in non-selective etching between the PI and PS blocks in the copolymer.

These results contrast with those of Harrison et al. [9], the only other published work that we know of concerning ozonation of diblock copolymers. They investigated PS rich block copolymers (i.e. the inverse composition to that here). For both a PS–PI diblock (85% PS, 15% PI) and a PS–PB diblock (77% PS, 23% PB) they observed selective etching, with the (minority) polydiene structures in the (majority) PS being removed. This was explained by the rate of cleaving of bonds in polystyrene being approximately one million times faster than for polyisoprene [26]. In our case the D1117 PS–PI block copolymer is rich in PI and this may account for the non selective chemical etching observed. The ozone dose used in our study, with 0.1% (wt/wt) ozone in the gas stream, is lower than that by employed by Harrison et al. (4% (w/w)). However, the duration of ozonation in our study was 80 min, considerably longer than the four minutes used by Harrison et al, making the total ozone dose supplied comparable. It is possible that

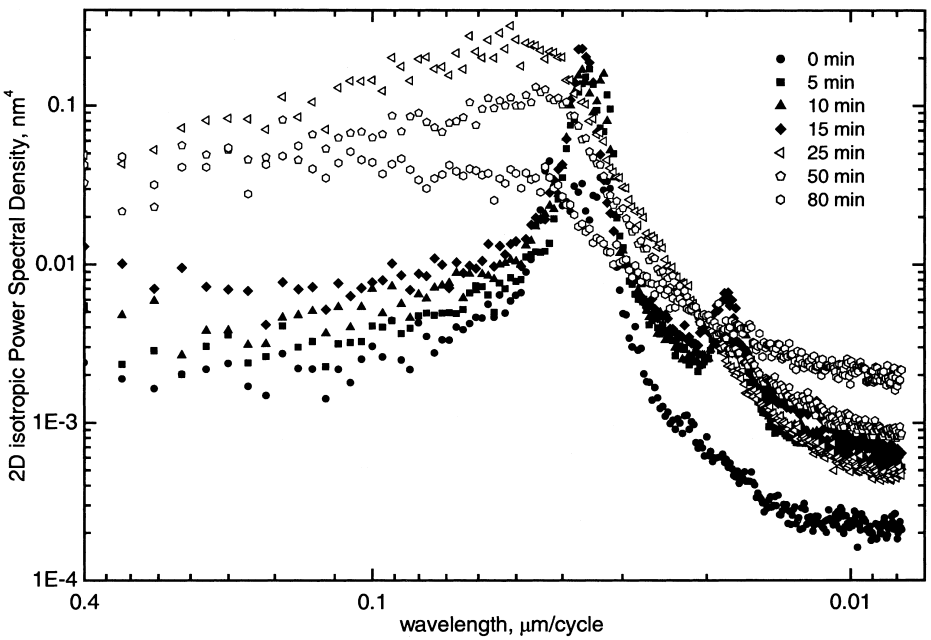

Fig. 6. 2D isotropic PSD display of the images in Fig. 4 (topographic AFM images of D1117 cast onto silicon after various times of ozonation).

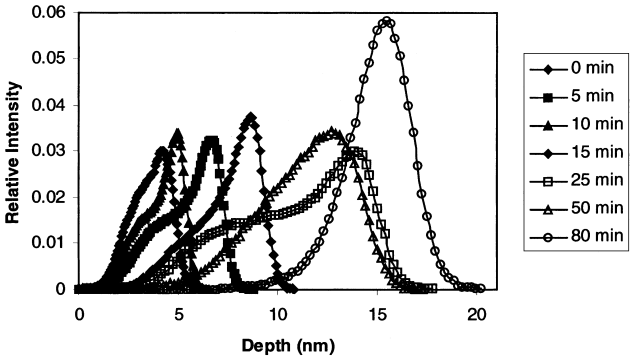

Fig. 7. Topographic AFM images of D1117 cast onto silicon after various times of ozonation (silicon was heat treated for 1 h at 1100 °C before casting, polymer was then annealed at 130 °C for 3 h before ozonation). (Data normalised to make area for each image the same.)

increasing the duration time and/or dose used may lead to selective etching.

4. Conclusions

The influence of ozonation on the morphology of thin films of a PS/PI block copolymer forming a stripe pattern was examined by AFM. Films were prepared on high surface energy silicon oxide layers to reduce dewetting on annealing the polymer films. The increase in surface energy was quantified through contact angle measurements, and the thickness through ellipsometry.

The effect of ozonation on the surface morphology was investigated via quantitative analysis of AFM images (height cross sections, PSDs and depth profiles). This revealed ozonation of the PS/PI sample studied (containing 83 wt% PI) led to non-selective etching for the ozone doses employed. This contrasts with prior results by Harrison et al. on samples where the diene component was the minority phase (23% PB in a PS–PB diblock or 15% PI in a PS–PI diblock) where selective etching was observed [9]. We conclude that the morphology has a profound effect on the ability to selectively etch a block copolymer film. In our case, we suppose that since the PS phase is dispersed, it cannot act to 'reinforce' the surface structure during etching and so the etching is non-selective.

Acknowledgements

We thank the EPSRC for supporting SC (grant GR/N00678) and TM (GR/N64793).

References

[1] Thurn-Albrecht T, Schotter J, Kästle GA, Emley N, Shibauchi T, Krusin-Elbaum L, Guarini K, Black CT, Tuominen MT, Russell TP. Science 2000;290:2126.
[2] Liu K, Baker SM, Tuominen M, Russell TP, Schuller IK. Phys Rev B 2001;63:060403(R).
[3] Cheng JY, Ross CA, Chan VZ-H, Thomas EL, Lammertink RGH, Vancso GJ. Adv Mater 2001;13:1174.
[4] Jeoung E, Galow TH, Schotter J, Bal M, Ursache A, Tuominen MT, Stafford CM, Russell TP, Rotello VM. Langmuir 2001;17:6396.
[5] Koslowski B, Strobel S, Herzog T, Heinz B, Boyen HG, Notz R, Ziemann P, Spatz JP, Möller M. J Appl Phys 2000;87:7533.
[6] Lopes WA, Jaeger HM. Nature 2001;414:735.
[7] Lopes WA. Phys Rev E 2002;65:031606.
[8] Park M, Harrison C, Chaikin PM, Register RA, Adamson DH. Science 1997;276:1401.
[9] Harrison C, Park M, Chaikin PM, Register RA, Adamson DH. J Vac Sci Technol B 1998;16:544.
[10] Hamley IW. The physics of block copolymers. Oxford: Oxford University Press; 1998.
[11] Matsen MW. Curr Opin Colloid Interface 1998;3:40.
[12] Fasolka MJ, Mayes AM. Annu Rev Mater Res 2001;31:323.
[13] Hamley IW. Angew Chem, Int Ed 2003; in press.
[14] Kraton, Kraton; 2002.
[15] Wu S. In: Brandrup J, Immergut EH, Grulke EA, editors. Polymer handbook, 4th ed. New York: Wiley; 1999.
[16] Knoll A, Magerle R, Krausch G. Macromolecules 2001;34:4159.
[17] Kraton Polymers data sheet, Shell Chemicals; 1997.
[18] van Dijk MA, van den Berg R. Macromolecules 1995;28:6773.
[19] Hattori T, editor. Ultraclean surface processing of silicon wafers secrets of VLSI manufacturing. Berlin: Springer; 1998.
[20] Thomas RR, Kaufman FB, Kirleis JT, Belsky RA. J Electrochem Soc 1996;143:643.
[21] Neumann AW, Good R. Surf Colloid Sci 1979;11:31.
[22] Owens DK, Wendt RC. J Appl Polym Sci 1969;13:1741.
[23] Solanky SS, Singh RP. Prog Rubber Plast Technol 2001;17:13.
[24] Palik ED, editor. Handbook of optical constants of solids. New York: Academic Press; 1985.
[25] Magerle R. Phys Rev Lett 2000;85:2749.
[26] Razumovskii SD, Kefeli AA, Zaikov GE. Eur Polym J 1971;7:275.